CGMS

CGMS-39 IOC-WP-01
16 September 2011
Prepared by NASA
Agenda Item: E.3
Discussed in Plenary

SEA SURFACE TEMPERATURE FOR NUMERICAL WEATHER PREDICTION

In response to CGMS action/recommendation A38.34

The atmosphere and oceans are joined together over seventy percent of Earth, with sea surface temperature (SST) one of the linkages. Sustained satellite SST measurements are critical for weather and climate applications. Small-scale SST gradients produced wind divergence and wind stress curl throughout the global marine atmospheric planetary boundary layer. Strong SST gradients enhanced deep convection throughout the troposphere. The international Group for High Resolution Sea Surface Temperature is working to improve the accuracy and resolution of SST used in atmospheric general circulation models, including numerical weather prediction models.

Action/Recommendation proposed: Improve accuracy of numerical weather prediction data products through utilization of satellite high-spatial resolution sea surface temperature data.

SEA SURFACE TEMPERATURE FOR NUMERICAL WEATHER PREDICTION

David Halpern[1]
Earth Science Division
NASA Headquarters
Washington, DC 20546, USA

1 INTRODUCTION

Sea surface temperature (SST) has an important influence on the atmosphere. It has long been known that high SST, generally above 26.5 °C, is required for convection that extends throughout the troposphere. The formation of tropical cyclones and hurricanes (Palmén, 1948) [Figure 1] is an example. The El Niño and La Niña phenomenon in the eastern equatorial Pacific Ocean is another example (Philander, 1990).

In the late 1980s, analyses of measurements from ships and from surface buoys moored to the ocean bottom at depths reaching 5 km revealed that southeast trade wind speeds exiting the eastern equatorial Pacific cold tongue increased in strength over warmer water (Hayes et al., 1989; Wallace et al., 1989). Surface wind speeds were lower over cool water and higher over warm water, i.e., variations of surface wind speed and SST were positively correlated. This air-sea interaction was different than the conventional wisdom of negative correlation, i.e., higher wind speeds were correlated with lower SST because of increased evaporation and because increased wind-generated vertical mixing in the ocean raised colder water to the surface.

Two primary mechanisms help explain wind speed changes forced by SST gradients (Small et al., 2008) [Figure 2]. An increase in SST reduces the static stability of the near-surface atmosphere, which intensifies vertical mixing that would bring faster-moving air aloft to the surface. Park and Cornillon (2002) demonstrated the impact of SST-generated static stability on surface wind acceleration/deceleration at strong SST gradients, including an approximate 25-km horizontal adjustment distance of the surface wind. In another process, barometric pressure above the sea surface would be higher over cooler water compared to that over warmer water, and this gradient over small distances, where the Coriolis effect would be negligible, would increase the ambient wind speed for winds blowing from cool to warm waters.

Wind speed acceleration generates horizontal divergence. When the surface wind blows from warmer water onto cooler water, wind speed decreases and the

[1]For this paper, David Halpern represents the Intergovernmental Oceanographic Commission (IOC) of the United Nations Educational, Scientific and Cultural Organization. IOC is a member of the Coordination Group for Meteorological Satellites (CGMS). The IOC and World Meteorological Organization Joint Technical Commission on Oceanography and Marine Meteorology (JCOMM) is supporting IOC in providing guidance to the CGMS, in accord with CGMS Action 38-34, on ocean activities through preparation of an annual report on a topic of relevance to JCOMM.

deceleration produces convergence. Winds blowing parallel to the SST gradient generate wind stress curl (Chelton et al., 2004; Park et al., 2006).

Analyses of high-spatial resolution United States (US) National Aeronautics and Space Administration (NASA) Quick Scatterometer ocean surface vector winds and NASA Tropical Rainfall Measurement Mission Microwave Imager SST data by Chelton et al. (2004) and Xie (2004) revealed previously unresolved wind stress curl and wind divergence features over the global oceans. At the Gulf Stream, where the SST gradient is quite large, Park and Cornillion (2002) had observed the linear coupling between SST gradient and wind speed. The small-scale near-surface curl and divergence characteristics of the near-surface wind field were each positively correlated with SST gradients [Figure 3]. Over most of the oceans where SST is less than 26.5 °C and SST gradients are relatively small, the SST-generated wind features are confined to the planetary boundary layer. However, strong SST fronts, like those at the edge of the Gulf Stream, influence not only the marine planetary boundary layer atmosphere (Song et al., 2006) but also the entire troposphere (Minobe et al., 2008) [Figure 4] through deep convection, even where SST is much lower than 26.5 °C.

Chelton and Xie (2010) found that a numerical weather prediction (NWP) model significantly underestimated the coupling between surface wind stress and SST compared to the observed relationship [Figure 3]. Atmospheric general circulation models underestimated the effects of SST on atmospheric circulation because model grid size is much larger than the horizontal dimension of the SST gradient (Minobe et al., 2008) [Figure 4] and/or the SST distribution does not accurately capture the small-scale SST gradients (Chelton and Wentz, 2005) [Figures 5, 6 and 7]. In the ocean, narrow-width (~ 100 km) currents and ubiquitous small-diameter (~ 10-50 km) eddy currents produce a wide range of small-scale SST gradients.

In addition to the resolution limitations of the SST boundary condition used in NWP models, the parameterization of vertical mixing in the models underestimates the sensitivity to stability in the lower marine atmospheric planetary layer (Song et al., 2009). As a result, global models underestimate the surface wind response to SST by about a factor of two (Song et al., 2009; Chelton and Xie, 2010).

2 SATELLITE SEA SURFACE TEMPERATURE MEASUREMENT CAPABILITY

The meaning of SST depends on measurement technology and strength of assumptions used to associate the measurement as a true representation of SST. For example, satellite infrared and microwave instruments measure SST to depths of 10^{-5} and 10^{-3} m, respectively, (Bertie and Lan, 1996) and a drifting surface buoy measures temperature at 0.2 - 0.3 m (http://www.aoml.noaa.gov/phod/dac/LumpkinPazos.pdf). A long-standing challenge continues to be the combination of SST measurements recorded from a variety of in-situ and satellite platforms, each with different space and time characteristics.

Prior to the advent of satellite SST measurements, SST gradients were estimated from sparsely sampled SST data recorded from ships. Monthly or annual mean variations were impossible to detect throughout most of the global ocean, although

adequate data were potentially recorded over the well-traveled portions of the North Atlantic, North Pacific and several coastal regions.

In July 1978, NASA launched the research SeaSat satellite with several different instruments, including a Scanning Multichannel Microwave Radiometer instrument that measured SST in the presence of clouds (Bernstein, 1982). Unless raining heavily, clouds do not attenuate microwave electromagnetic radiation emitted from the sea surface at the frequencies used to measure SST. The SeaSat satellite had a catastrophic failure in October 1978.

In October 1978, NASA launched the operational Television Infrared Observation Satellite (TIROS-N [N=NOAA, US National Oceanic and Atmospheric Administration]) satellite with several different instruments, including the first in a multi-decade series of Advanced Very-High Resolution Radiometer (AVHRR) instruments that measure SST (Legeckis and Cresswell, 1981) in clear-sky conditions. Aerosols degraded the AVHRR infrared radiation measurement, and clouds obscure the seas surface from infrared measurements. At any moment in time, the sky is cloudless over about 50% of the surface of the global ocean (Platnick et al., 2003; Wylie et al., 2005), although over large oceanic areas the clear-sky fraction is about 25%. Any infrared SST pixel with some cloud, maybe only over a few percent of the pixel area, is identified and removed from further data processing; this stringent requirement leads to 85-90% of the sea surface rejected by cloud screening algorithms. In Figures 5, 6 and 7, the presence of clouds caused the absence of AVHRR SST data but clouds did not interfere with corresponding Advanced Microwave Scanning Radiometer SST measurements.

2.1 GROUP FOR HIGH RESOLUTION SEA SURFACE TEMPERATURE

Many currently operating satellites have infrared and microwave instruments to record SST (Donlon et al., 2007), and multiple global SST data sets are produced throughout the world. The Global Ocean Data Assimilation Experiment (http://www.godae.org/index.htm) High Resolution Sea Surface Temperature (GHRSST), now called the Group for High Resolution Sea Surface Temperature (https://www.ghrsst.org/), is the international expert group for the coordination, provision and application of high accuracy SST data to operational and research communities. Through the NASA Jet Propulsion Laboratory Physical Oceanography Distributed Active Archive Center and other portals, GHRSST offers a suite of global high-resolution SST products, operationally, in near-real time, on a daily basis. GHRSST harmonizes diverse satellite and in-situ data with error estimates that are indexed, processed, quality controlled, analyzed, and documented within an international framework. Each day, GHRSST produces a multi-product ensemble median average SST distribution (http://ghrsst-pp.metoffice.com/pages/latest_analysis/sst_monitor/daily/ens/index.html) for the previous day at 1200 GMT on a 0.5-degree latitude by 0.5-degree longitude grid (Martin et al., submitted) [Figure 8]. Currently, 11 GHRSST data products are utilized [Table 1]. The corresponding standard deviation and the differences between each product and ensemble-mean product are also distributed (http://ghrsst-pp.metoffice.com/pages/latest_analysis/sst_monitor/daily/ens/index.html). Many GHRSST data sets have smaller grid dimensions than 0.5 degree. Because of cloud cover limitations in the availability of infrared measurements of SST, the feature

resolution of the SST fields in the various GHRSST data products is generally much coarser than the grid dimensions (Reynolds and Chelton, 2010); for clear-sky conditions, the feature resolution of infrared SST data is generally that of the 4-km grid resolution. For microwave SST data, the grid resolution is about 25 km, although the resolution of the underlying data is closer to 50 km.

A GHRSST Science Team co-ordinates data production, ease of access, user guidance, and related research and development, with special foci on efforts to resolve diurnal variability, skin temperature deviation, and validation of the GHRSST products, as well as on improving retrieval algorithms and historical re-analysis. Activities occur on assessing the resolution limitations of currently available SST analyses (Reynolds and Chelton, 2010), which is extremely important to utilize thirty years of AVHRR data for climate studies. Vazquez-Cuervo et al. (2010) found that the magnitudes of climatological-mean monthly SST gradients in the Gulf Stream and California coastal region were 50% larger in 4-km infrared SST data than in 9-km data.

Major stakeholders are represented in the GHRSST Advisory Council, which advises the GHRSST Science Team on its strategy. A GHRSST Project Office, currently located at the United Kingdom National Centre for Earth Observations, supports the smooth day-to-day working of the group. The Committee on Earth Observation Systems (CEOS) considers GHRSST to be the CEOS SST Virtual Constellation (https://www.ghrsst.org/documents/q/category/ceos-sea-surface-temperature-virtual-constellation-sst/).

Target accuracies for GHRSST data are 0.3 °C absolute, 0.1 °C relative and 1-km in position, with a temporal stability of 0.01 °C per decade (https://www.ghrsst.org/ghrsst-science/science-team-groups/ran-tag/latest-climate-record-requirements/). The quality of satellite SST retrievals depends critically on the availability of high accuracy, well-calibrated, stable in-situ SST datasets. The most useful component of the current in situ SST observing system is a fleet of about 1500 surface buoys freely drifting throughout the global oceans (Corlett et al., 2006). The JCOMM Data Buoy Co‑operation Panel (DBCP) coordinates the operation and maintenance of the drifter fleet. In 2010, the DBCP and GHRSST initiated a joint project to improve the accuracy of drifting buoy temperature and location measurements (https://www.ghrsst.org/documents/q/category/argo-dbcp-and-sot/jcomm-dbcp-ghrsst-pilot-project/).

Many satellites record SST. A December 2010 inventory of satellite SST measurement capabilities shows that 20 satellites (some with multiple instruments that measure SST) are currently in orbit and 9 satellite missions have been approved for launch by 2025 (Initial SST-VC Proposal Submitted to CEOS-SIT 14 Dec 10, https://www.ghrsst.org/documents/q/category/ceos-sea-surface-temperature-virtual-constellation-sst/). To maximize the impact and benefit of existing and future SST measurements from all in-situ platforms, GHRSST recommended in April 2011 that JCOMM (https://www.ghrsst.org/files/download.php?m=documents&f=110718164621-GHRSSTXIIBartonReport.pdf):

> Add the provision of radiometric skin SST data and radiosonde capability to its portfolio of Volunteer Observing Ship measurements.
>
> Ensure that ships and other platforms currently providing high quality in-situ SST

data where possible expand their provision of near-surface temperature profiles, wind speed, history of wind speed, air temperature and humidity.
Enhance the capability of Argo floats, drifting buoys and moorings to measure temperature profiles in the uppermost 2 meters of the ocean.
Calibrate in-situ instrumentation, preferably against a standard traceable to a SI reference.
Establish a working group to collaborate with GHRSST to better define requirements for SST measurements from marine platforms, and to identify new opportunities that may assist with a more uniform coverage of the global oceans.
Enable ship of opportunity participation in future SST measurement inter-comparison tests.
Use GHRSST data to assess the accuracy and performance of SST measurements.

2.2 IOC REQUIREMENTS FOR SATELLITE SST MEASUREMENTS

The IOC exists for coordination and joint work between its Member States of ocean science, observations, and services. IOC is the lead sponsor for the Global Ocean Observing System (GOOS) and co-sponsor of JCOMM and Global Climate Observing System (GCOS).

GOOS is a voluntary collaborative system of ocean observing networks responding to high-level requirements for climate monitoring, weather forecasting, and ocean-related hazard warning. It is increasingly identifying new requirements for ocean observations for management and stewardship of the ocean environment. SST is an essential requirement expressed for many of these applications.

IOC requirements for satellite SST measurements are developed in two processes:
GCOS for climate applications (9 May 2011 Draft Version 1.1; http://www.google.com/search?client=safari&rls=en&q=GCOS+Systematic+observation+requirements+for+satellite+based+products+for+climate+2011+update&ie=UTF-8&oe=UTF-8)
WMO Rolling Requirements Review for non-climate applications (http://www.wmo.int/pages/prog/sat/documents/RRRprocess.pdf) process.

3 CONCLUSIONS

A proper representation of small-scale SST gradients is critical for understanding the coupling of the atmosphere and ocean. Currently, NWP forecasts underestimate the surface wind response to SST and therefore the tropospheric response to SST. The NWP forecasts thus yield underestimates of surface heat and momentum fluxes, which then results in incorrect forcing fields of ocean general circulation models. GHRSST working together with JCOMM therefore offers opportunities for NWP centers to improve the forecast of the general circulation of the atmosphere as well as the ocean.

ACKNOWLEDGEMENTS

I am grateful to Dr. Dudley Chelton (Oregon State University), Dr. Peter Cornillon (University of Rhode Island), Dr. Albert Fisher (IOC), Dr. Eric Lindstrom (NASA Headquarters), and Dr. Peter Minnett (University of Miami) for insightful comments on early versions of the manuscript. Dr. Chelton kindly provided original versions of Figures 2, 3, 5, 6 and 7 and Dr. Lindstrom. I am indebted to Dr. Jack Kaye (NASA Headquarters) for his tremendous support for my participation in CGMS and JCOMM. The kind invitations by Dr. Albert Fisher (IOC) and the JCOMM Management Committee, led by Dr. Peter Dexter (Australia Bureau of Meteorology), to participate in CGMS are greatly appreciated.

Table 1. August 2011 components of GHRSST median ensemble average global SST distribution.

United Kingdom Meteorological Office Operational Sea Surface Temperature and Sea Ice Analysis (http://ghrsst-pp.metoffice.com/pages/latest_analysis/ostia.html)

United States National Center for Environmental Prediction Real-time Global Sea Surface Temperature Analyses (http://polar.ncep.noaa.gov/sst/)

United States Naval Oceanographic Office Level 4 K10_SST Global 1 Meter SST Analysis (http://podaac.jpl.nasa.gov/dataset/NAVO-L4HR1m-GLOB-K10_SST)

Japan Meteorological Agency Merged satellite and in situ Global Daily Sea Surface Temperatures (http://goos.kishou.go.jp/rrtdb/mgdsst.html)

Remote Sensing Systems Microwave Sea Surface Temperature (http://www.ssmi.com/sst/sst_data_daily.html?sat=tmi_amsre)

Remote Sensing Systems Microwave and Infrared Sea Surface Temperature (http://www.ssmi.com/sst/sst_data_daily.html?sat=mw_ir)

United States Navy Fleet Numerical Meteorology and Oceanography Center High Resolution SST/Sea Ice Analysis for GHRSST (http://www.usgodae.org/cgi-bin/datalist.pl?summary=Go&dset=fnmoc_ghrsst)

European Union Marine Environment and Security for the European Area Ocean Data analysis System for merSea (http://cersat.ifremer.fr/data/discovery/by_parameter/sea_surface_temperature/odyssea_global_sst_analysis)

United States National Oceanic and Atmospheric Administration Optimum Interpolation ¼ Degree Daily Sea Surface Temperature Analysis (http://www.ncdc.noaa.gov/oa/climate/research/sst/oi-daily.php)

Canadian Meteorological Center Sea Surface Temperature Analysis (https://www.ghrsst.org/files/download.php?m=documents&f=110627101605-L4summarytemplateCMC.doc)

Australia Bureau of Meteorology Global Australian Multi-Sensor Sea Surface

Temperature Analysis (http://www.bom.gov.au/australia/charts/bulletins/apob77.pdf)

REFERENCES

Bernstein, R. L. (1982) Sea surface temperature mapping with the SeaSat microwave radiometer. *Journal of Geophysical Research*, *87*, 7865-7872.

Bertie, J. E. and Z. Lan (1996) Infrared intensities of liquids XX: The intensity of the OH stretching band of liquid water revisited, and the best current values of the optical constants of H_2O at 25 °C between 15,000 and 1 cm^{-1}. *Applied Spectroscopy*, *50*, 1047-1057.

Chelton, D. B., M. G. Schlax, M. H. Freilich and R. F. Milliff (2004) Satellite measurements reveal persistent small-scale features in ocean winds. *Science*, *303*, 978-983.

Chelton, D. B. and F. J. Wentz (2005) Global microwave satellite observations of sea surface temperature for numerical weather prediction and climate research. *Bulletin of the American Meteorological Society*, *86*, 1097-1115.

Chelton, D. B. and S.-P. Xie (2010) Coupled ocean-atmosphere interaction at oceanic mesoscales. *Oceanography*, *23*(4), 52-69.

Corlett, G. K. and 15 co-authors (2006) The accuracy of SST retrievals from AATSR: An initial assessment through geophysical validation against in situ radiometers, buoys and other SST data sets. *Advances in Space Research*, *37*, 764-769.

Donlon, C. and 25 co-authors (2007) The Global Ocean Data Assimilation Experiment high-resolution sea surface temperature pilot project. *Bulletin of the American Meteorological Society*, *88*, 1197-1213.

Hayes, S. P., M. J. McPhaden and J. M. Wallace (1989) The influence of sea-surface temperature on surface wind in the eastern equatorial Pacific: weekly to monthly variability. *Journal of Climate*, *2*, 1500-1506.

Legeckis, R. and G. Cresswell (1981) Satellite observations of sea surface temperature fronts off the coast of western and southern Australia. *Deep-Sea Research*, *28*, 297-306.

Martin, M. J. and 14 co-authors (submitted) Group for High Resolution SST (GHRSST) Analysis Fields Inter-Comparisons: Part 1. A GHRSST Multi-Product Ensemble (GMPE). Submitted to *Deep Sea Research II*.

Minobe, S., A. Kuwano-Yoshida, N. Komori, S.-P. Xie and R. J. Small (2008) Influence of the Gulf Stream on the troposphere. *Nature*, *23*, 3699-3719.

Palmén, E. (1948) On the formation and structure of tropical hurricanes. *Geophysica*, *3*, 26-38.

Park, K.-A. and P. C. Cornillon (2002) Stability-induced modification of surface winds over Gulf Stream rings. *Geophysical Research Letters*, *29*, doi:10.1029/2001GL014236.

Park, K.-A., P. Cornillion and D. L. Codiga (2006) Modification of surface winds near ocean fronts: Effects of Gulf Stream rings on scatterometer (QuikSCAT, NSCAT) wind observations. *Journal of Geophysical Research*, *111*, doi:10.1029/2005JC003016.

Philander, S. G. H. (1990) *El Niño, La Niña, and the Southern Oscillation*. Academic Press, New York, 289 pp.

Platnick, S. and 6 co-authors (2003) The MODIS cloud products: Algorithms and example from Terra. *IEEE Transactions on Geosciences and Remote Sensing*, *41*, 459-474.

Reynolds, R. W. and D. B. Chelton (2010) Comparisons of daily sea surface temperature analyses for 2007–08. *Journal of Climate*, *23*, 3545-3562.

Ropelewski, C. F. and M. S. Halpert (1987) Global and regional precipitation patterns associated with the El Niño/Southern Oscillation. *Monthly Weather Review*, *115*, 1606-1626.

Small, R. J. and 8 co-authors (2008) Air-sea interaction over ocean fronts and eddies. *Dynamics of Atmospheres and Oceans*, *45*, 274-319.

Song, Q. , P. Cornillon and T. Hara (2006) Surface wind response to oceanic fronts., Journal of Geophysical Research, 111, C12006, doi:10/1029/2006JC003680.

Song, Q., D. B. Chelton, S. K. Esbensen, N. Thum, and L. W. O'Neill (2009) Coupling between sea-surface temperature and low-level winds in mesoscale numerical models. *Journal of Climate*, *22*, 146-164.

Vazquez-Cuervo, J. and 5 co-authors (201) Comparison between the Pathfinder versions 5.0 and 4.1 sea surface temperature datasets: A case study for high resolution. *Journal of Climate*, *23*, 1047-1059.

Wallace, J. M., T. P. Mitchell and C. Deser (1989) The influence of sea surface temperature on surface wind in the eastern equatorial Pacific: Seasonal and interannual variability. *Journal of Climate*, *2*, 1492-1499.

Wylie, D., D. L. Jackson, W. P. Menzel and J. J. Bates (2005) Trends in global cloud cover in two decades of HIRS observations. *Journal of Climate*, *18*, 3021-3031.

Xie, S.-P. (2004)Satellite observations of cool-atmosphere interaction. *Bulletin of the American Meteorological Society*, *85*, 195-208.

Principal Hurricane Paths and SST During Warmest Season)

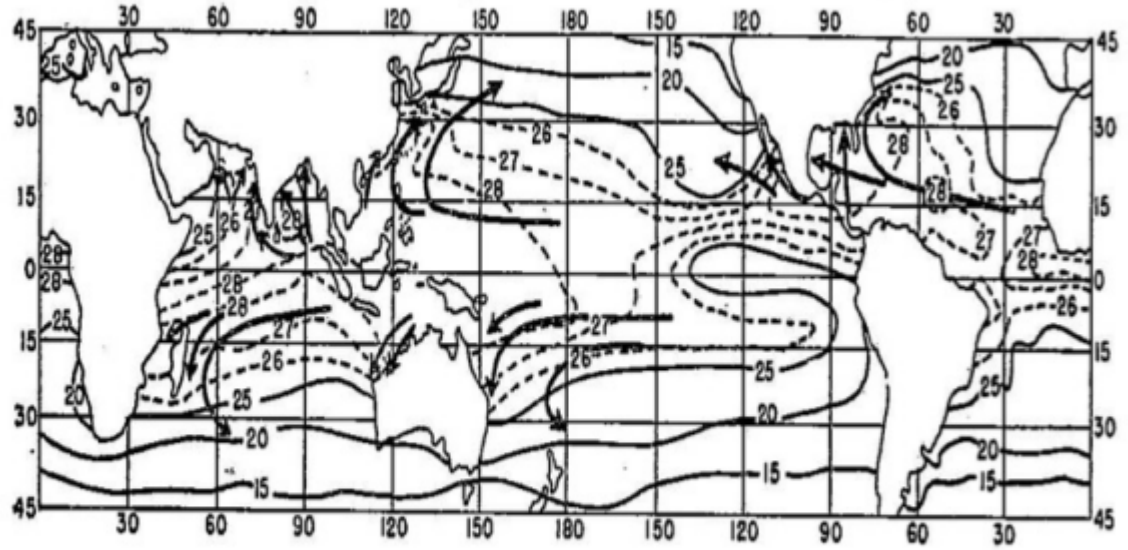

Hurricanes form only in oceanic regions outside the vicinity of the equator where SST > 26-26 °C.

A strong vortex can form in the area of converging air when $|f|$ > critical value and $f = 0$ at the equator.[1]

Palmén (1948)

FIGURE 1

Divergence and Curl of the Wind Generated by SST Gradients

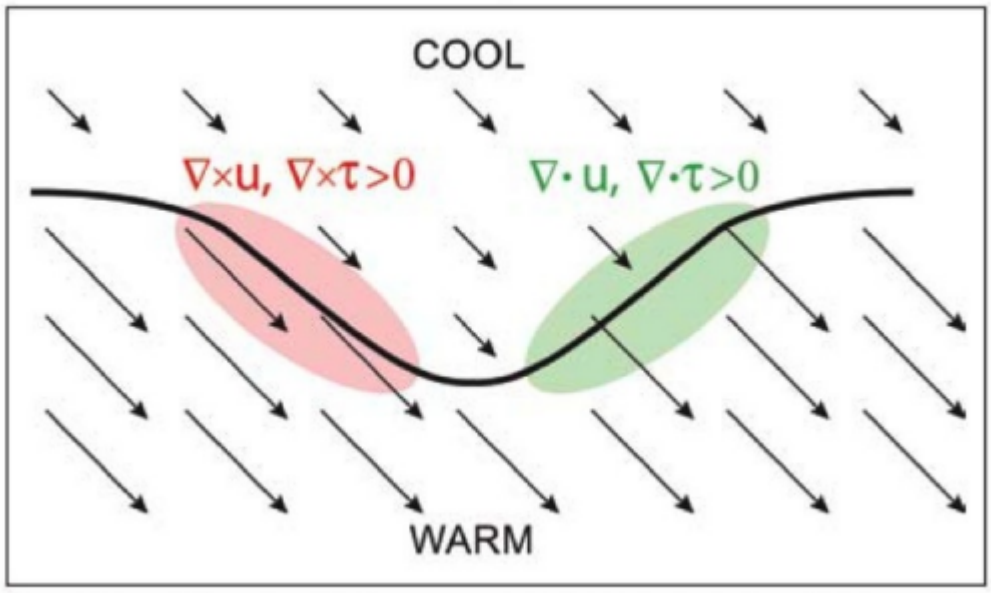

[2]

Chelton and Xie (2010)

FIGURE 2

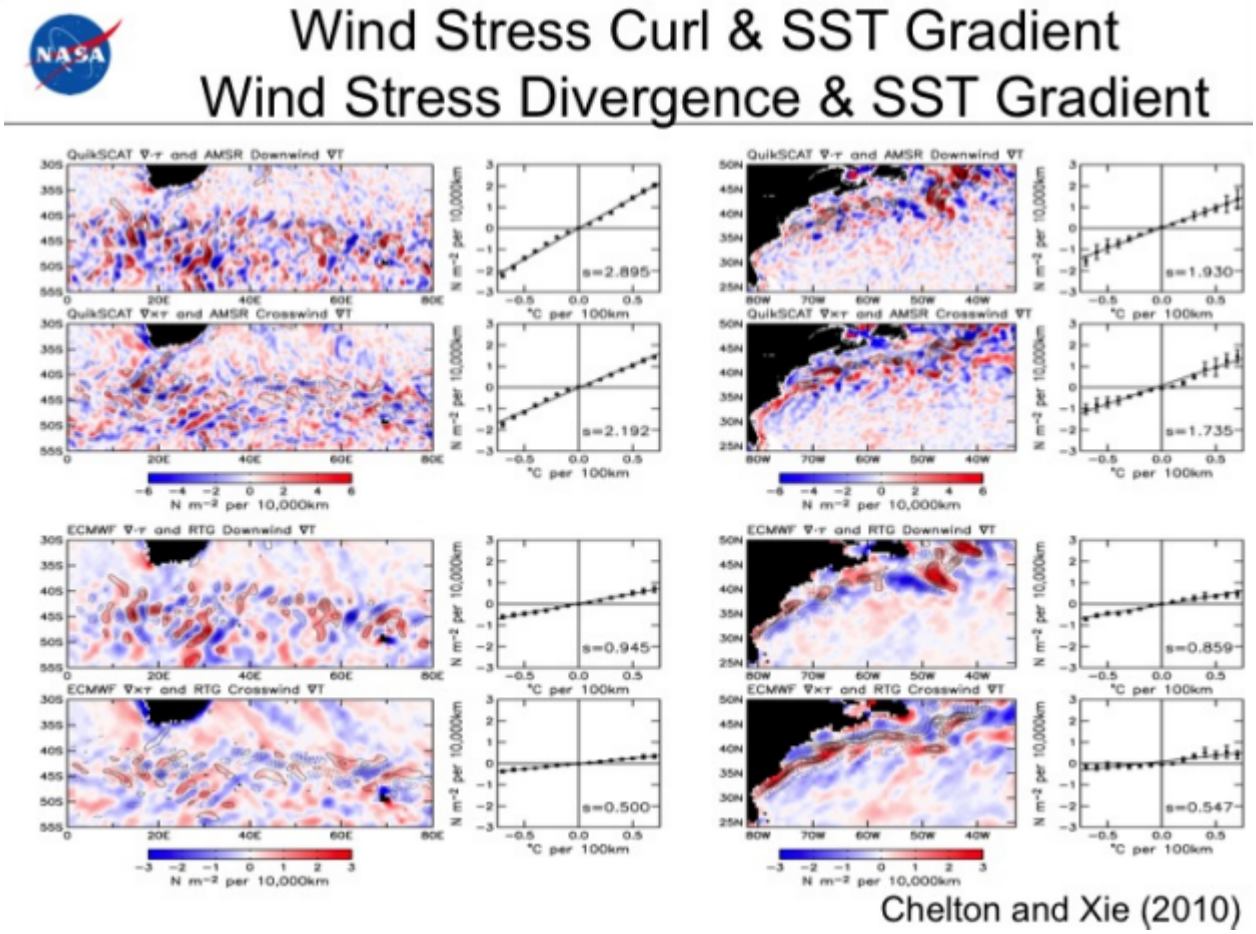

FIGURE 3

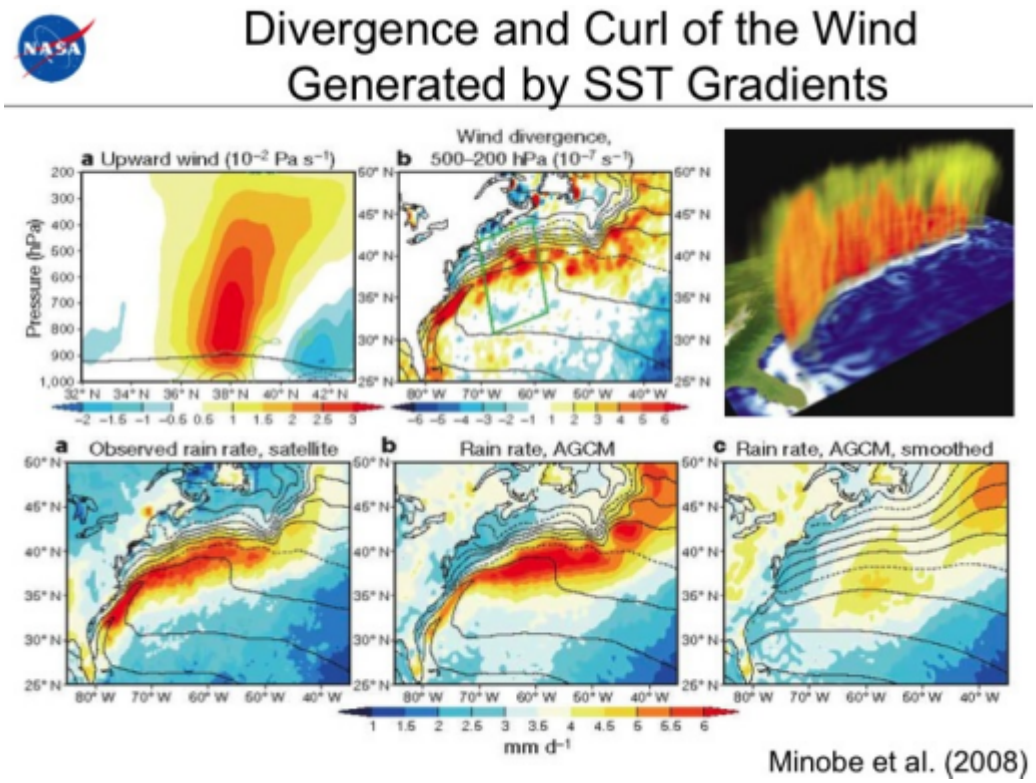

FIGURE 4

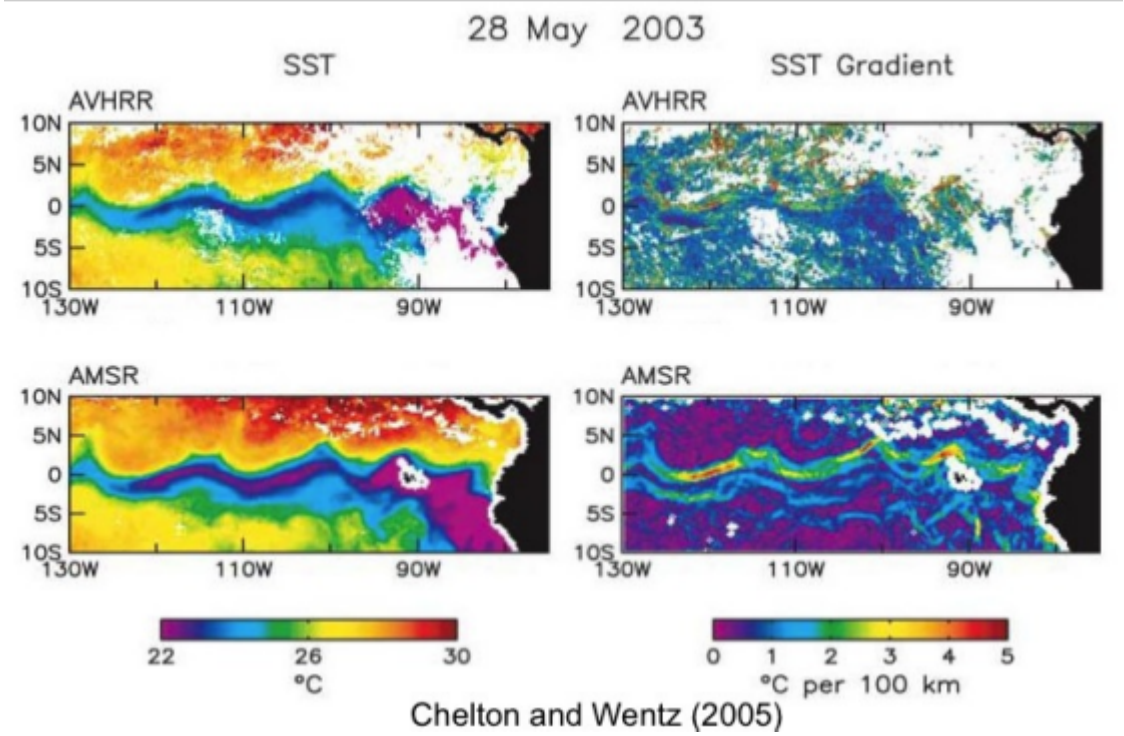

FIGURE 5

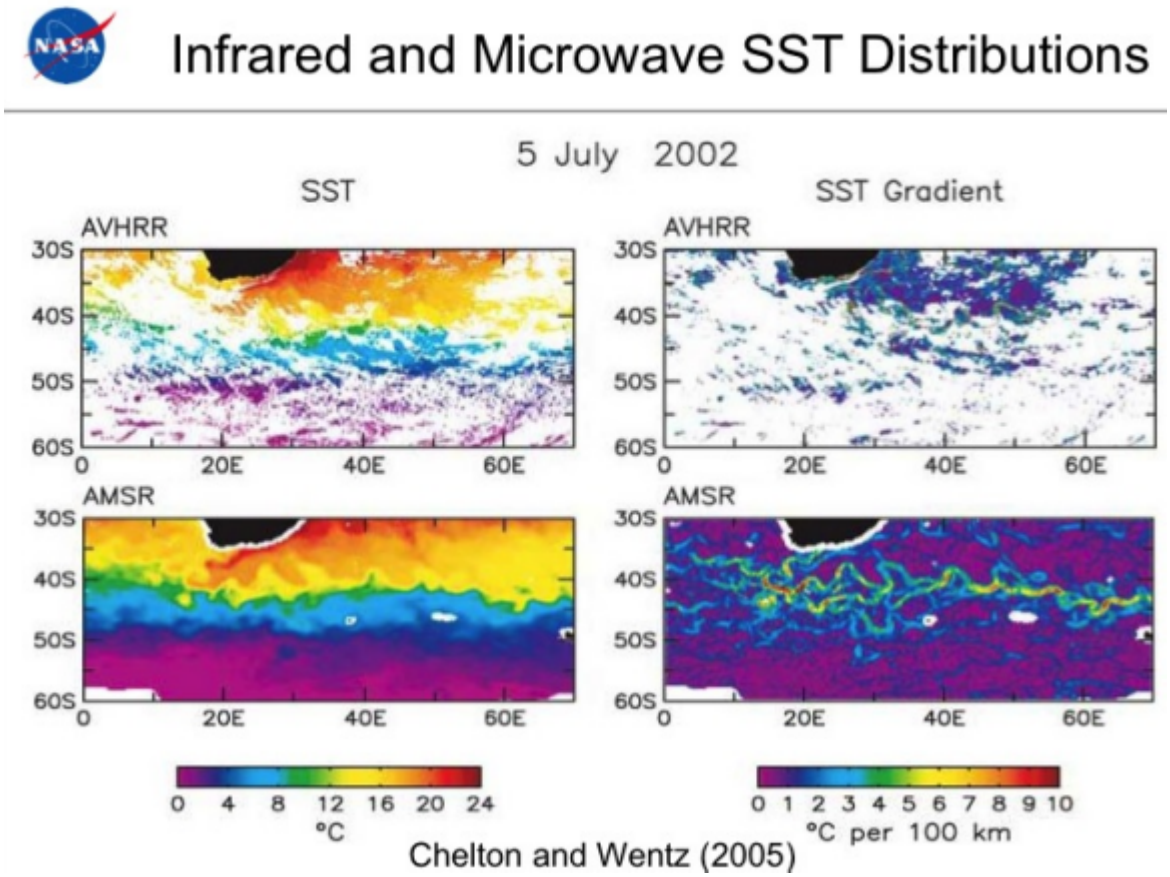

FIGURE 6

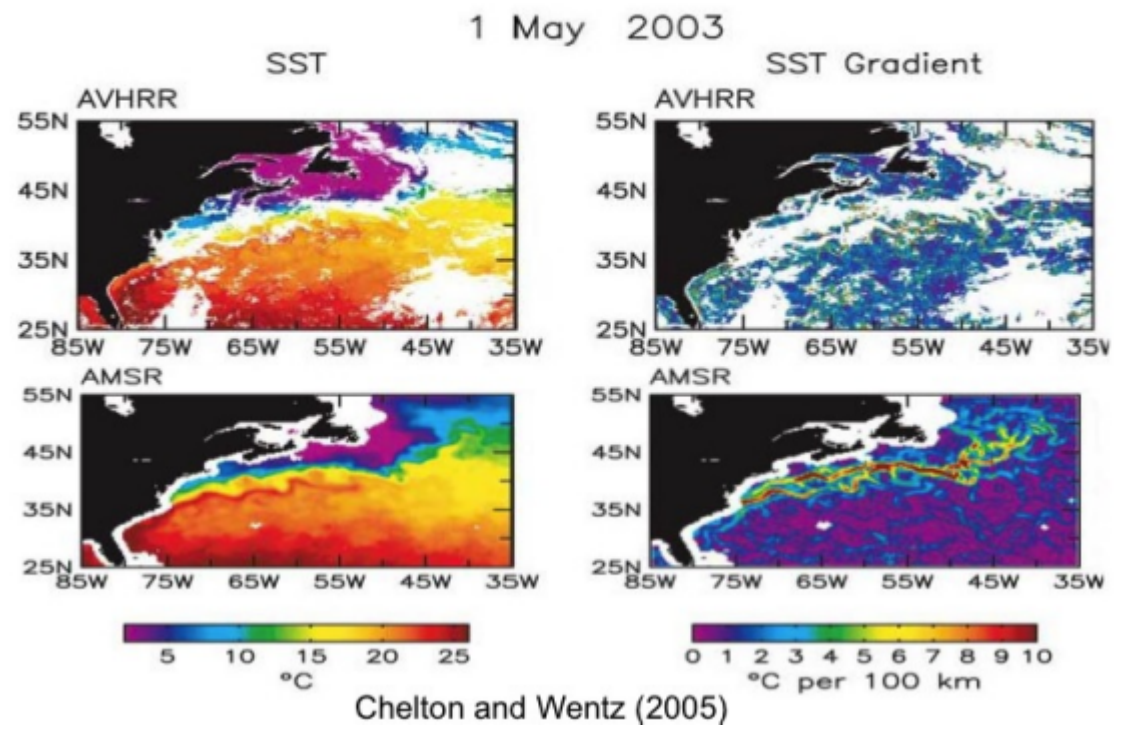

FIGURE 7

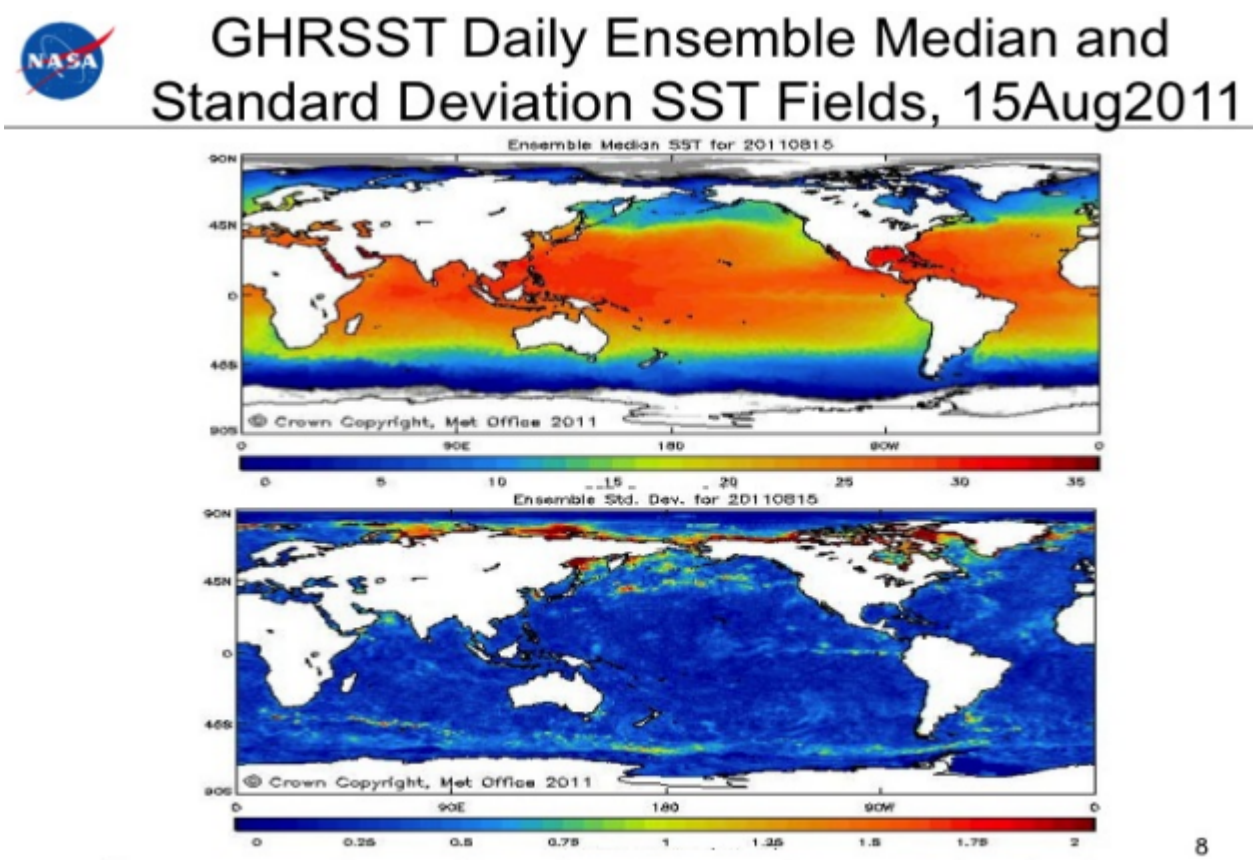

FIGURE 8